

Recent Advancements in Electrode Materials for the High-performance Electrochemical Supercapacitors: A Review

Shen-Ming Chen^{1,*}, Rasu Ramachandran², Veerappan Mani¹, Ramiah Saraswathi²

¹ Electroanalysis and Bioelectrochemistry Lab, Department of Chemical Engineering and Biotechnology, National Taipei University of Technology, No.1, Section 3, Chung-Hsiao East Road, Taipei 106, Taiwan (ROC).

² Department of Materials Science, School of Chemistry, Madurai Kamaraj University, Madurai-625 021, Tamil Nadu, India.

*E-mail: smchen78@ms15.hinet.net

Received: 18 October 2013 / Accepted: 5 November 2013 / Published: 19 May 2014

Supercapacitors are energy storage devices emerging as one of the promising energy storage devices in the future energy technology. In this perspective, rapid progress is made in the development of fundamental and applied aspects of supercapacitors. Various techniques have been developed specifically to estimate the specific capacitance. Numerous efforts were made in the literature to increase the specific capacitance value of the electrode materials. The electrode materials which have unique structural and electrochemical capacitance properties, such as high capacity and cyclic stability showed great supercapacitors performances. Recently, there are much new types of electrode materials were developed to play an important role in the capacitance behavior. In this review, we focused on the applications of various nanostructured electrode materials like carbon nanomaterials, metal oxides and conducting polymer towards highly efficient supercapacitors.

Keywords: Carbon based materials, metal oxides, conducting polymers, supercapacitors

1. INTRODUCTION

Increasing demand in the need of global-energy drives the development of alternative or non-conventional energy sources with high power and energy densities [1]. Batteries, fuel cells and supercapacitors are typical non-conventional energy devices which are based on the principle of electrochemical energy conversion. They find widespread applications in consumer electronics ranging from mobile phones, laptops, digital cameras, emergency doors and hybrid vehicles etc. [2]. In these devices, chemical energy is converted in to electrical energy by means of electrochemical reactions. As

far the fuel cells are concerned, as long as the fuel is fed, electrical energy can be obtained. In case of batteries, the stored energy can be drawn at the time of need. Supercapacitor is a typical energy storage device (similar to secondary battery) which possess high specific capacitance, high power density and long cycle life [3]. Supercapacitors can be used in combination with batteries to meet the start-up power, usually high power density. Depending on the mode of energy storage in supercapacitors, they are classified as in to electrical double layer capacitors (EDLC) and pseudo-capacitors or ultra capacitors [4]. Charge accumulation at the vicinity of electrode/electrolyte occurs in the case of electrical double layer capacitor (EDLC), whereas charge transfer across the electrode/electrolyte interface takes place in the latter case [5]. On the one hand, EDLC offer high power density than the redox capacitors due to the large charge accumulation. On the other hand, the redox capacitors offer high energy density due to large potential window than the EDLC.

The major classes of active electrode materials used for the supercapacitors such as, activated nanoporous carbon [6], carbon aerogel [7], carbon nanosheets [8], carbon nanotubes [9], conducting polymers [10], metal oxides [11] and polymer composites [12,13,14] have been extensively examined and reported in literature till date. Conducting polymer is one of the promising electrode materials for the supercapacitors applications. It gives large number of charge/discharge cycles and exhibits high specific capacitance properties. For instance, polyaniline, polythiophene, poly-(3,4-ethylenedioxythiophene) and polypyrrole are the major polymers employed for the supercapacitors applications. Recently, graphene modified electrodes such as graphene-MnO₂ [15], graphene-ZnO [16], exfoliated graphite-RuO₂ [17] and graphene-CNT [18] composites were used as energy storage devices for the supercapacitors applications.

2. CLASSIFICATIONS OF SUPERCAPACITORS

Generally supercapacitors are classified into the following two types:

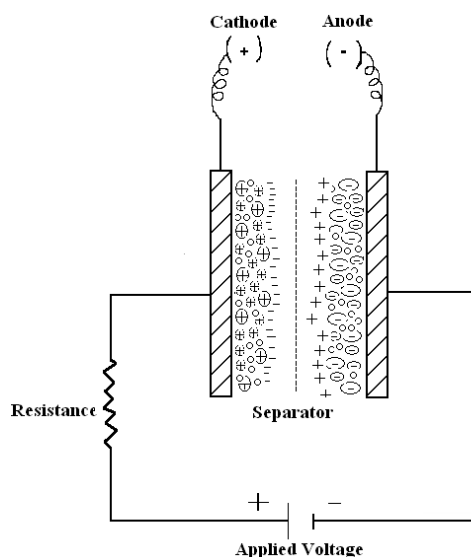


Figure 1. Schematic representation of electrochemical supercapacitors

2.1. Electrical double-layer capacitor

It is a combination of two carbon based electrode materials separated by an insulator (shown in Fig.1). It stores the energy charge by non-faradaic manner and there is no charge transfer at electrode-electrolyte interface. Carbon nanomaterials are unique structures with large surface area, high chemical, mechanical stability and excellent electrical conductivity.

2.2. Pseudo-capacitors

Pseudo-capacitors electrostatically store the charge and the faradaic charge transfer occurs at electrode-electrolyte interface. It has high specific capacitance and high energy density than the electrical double layer capacitance. Transition metal oxides [19, 20] and conducting polymers [21, 10, 22] are good examples of pseudo-capacitors or redox capacitors. RuO₂ stands as best electrode material for the pseudo-capacitor applications than the other metal oxides.

3. DIFFERENT TECHNIQUES FOR THE ANALYSIS OF SUPERCAPACITORS

Cyclic voltammetry, Galvanostatic charge/discharge and Electrochemical Impedance methods are the important techniques usually employed to analyze the newly fabricated supercapacitors.

3.1. Cyclic voltammetry

The pseudo-capacitance of metal oxides and conducting polymers has been evaluated by cyclic voltammetry (CV) method. CVs were recorded at traditional three electrode system consisting of working electrode, counter electrode and reference electrode in appropriate supporting electrolytes at various scan rates.

It can estimate the value of specific capacitance of the particular modified and unmodified electrode materials analyzed. The voltammetry responses of synthesized nanomaterials were carried out at different scan rates. The specific capacitance performance in various electrolytes (acidic or alkaline) were carried out in their corresponding potential range (in volts, V) and recorded at various sweep rates (mV s⁻¹). It was interpreted that, when the scan rate increases the value of specific capacitance decreases and this trend have already been described by Li *et al* [23]. The following equation (1) has been used to calculate the specific capacitance value by using cyclic voltammetry method [19, 24, 25].

$$C_{cv} = \frac{1}{2m\Delta V} [Q_a + Q_c] \text{ F g}^{-1} \quad (1)$$

Using the working electrode, the average specific capacitance value can be estimated from anodic charge (Q_a) and cathodic charge (Q_c) in one cycle of potential sweep, where m is the weight of deposited electrode material.

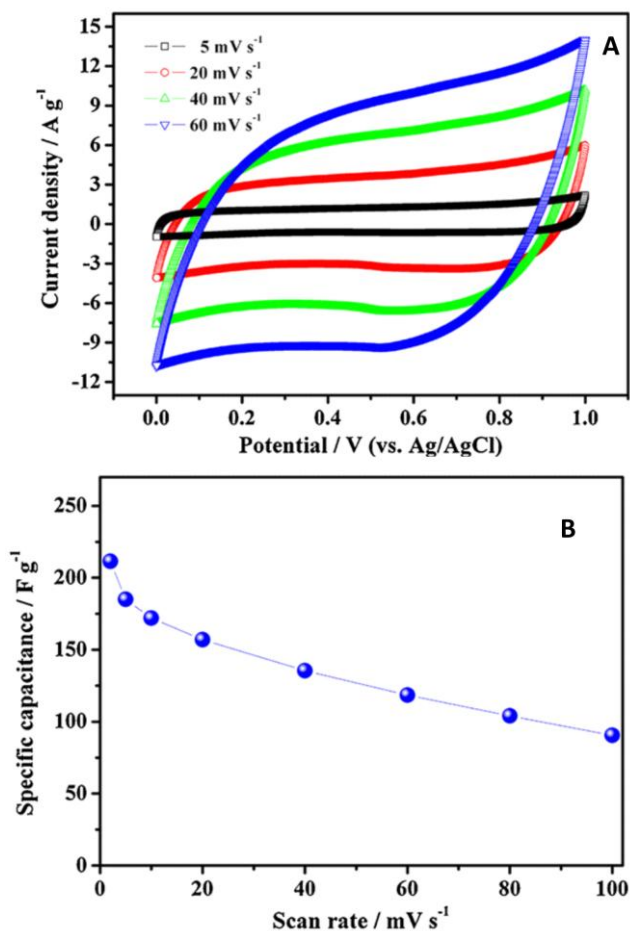


Figure 2. (a) Cyclic voltammograms of hydrothermally reduced graphene/MnO₂-200 electrode at different scan rates in 1M Na₂SO₄ electrolyte; (b) the specific capacitance as a function of potential scan rates (Reproduced with permission from ref. [27]).

Liu *et al* [26] used the voltammetry technique to estimate specific capacitance value. Li *et al* [27] used hydrothermally reduced graphene/MnO₂-200 composite electrode by cyclic voltammetry technique, which was recorded at various scan rates (5 - 60 mV s⁻¹) to estimate the respective capacitance values. The authors were reported that lower scan rate exhibited higher capacitance value than higher scan rates as shown in fig. 2.

3.2. Pseudo-capacitance examined by charge/discharge method

The charge/discharge behavior of the electrodes was examined by chronopotentiometry method. It was carried out at a supporting electrolyte (acidic or alkaline) between initial potential to final potential at a particular current density. From the charge/discharge method, it was observed that the charging curves were almost similar to discharging curve, but slightly differs from the initial charging time. The average specific capacitance of the deposited electrode materials (carbanous materials, metal oxide and conducting polymer) can be evaluated from the following equation (2) [28-30].

$$C_{cp} = \frac{I \times \Delta t}{\Delta V \times m} F g^{-1} \quad (2)$$

Where, I is the discharging current (A), Δt is the discharging time, ΔV is the discharging voltage and m is the mass of active material.

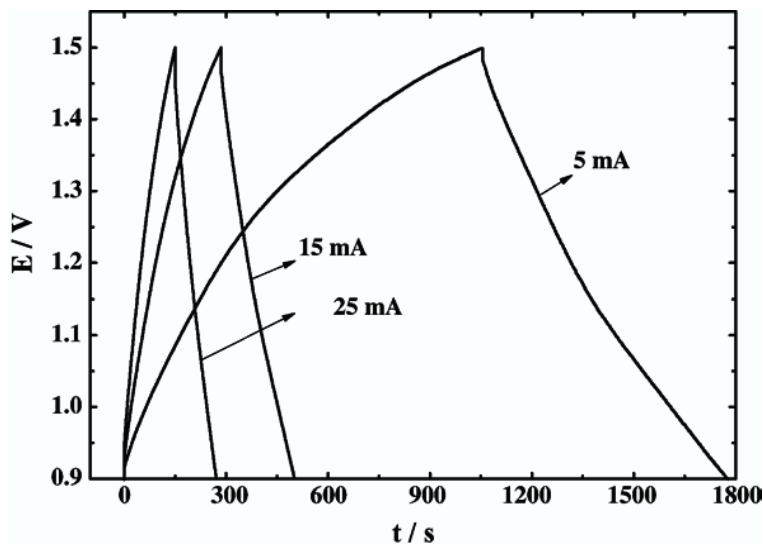


Figure 3. Charge/discharge curves of hybrid supercapacitor at different currents (Reproduced with permission from ref. [35]).

When both the techniques were compared, (charge-discharge and cyclic voltammetry) specific capacitance values were almost reliable. A slight variation in potential observed on the start of the discharge curve is due to the IR drop at each half-cycle, which dramatically reduces the power and capacity [31]. The charge-discharge behaviors of the active electrode materials were recorded at different current densities using current density as one of the parameter [32-34] within an applied potential window and appropriate supporting electrolyte. For instance, the galvanostatic charge-discharge curves of hybrid capacitor were recorded at various current densities like 5 mA, 15 mA and 25 mA [35] as represented in fig. 3. This technique has been used to study the stability of electrode materials. The charge/discharge test of the electrode was carried out up to 1000 cycles and the capacitance dropped by only 10 % leading to the interpretation that this type of electrode materials has good electrode stability [36]. On the other hand, the electrode material for which the capacitance value dropped in the order of 40 to 50 % has rated to be less stable electrodes.

3.3. Electrochemical impedance spectroscopy

Electrochemical impedance spectroscopy is one of the techniques, which has been used to evaluate the specific capacitance values.

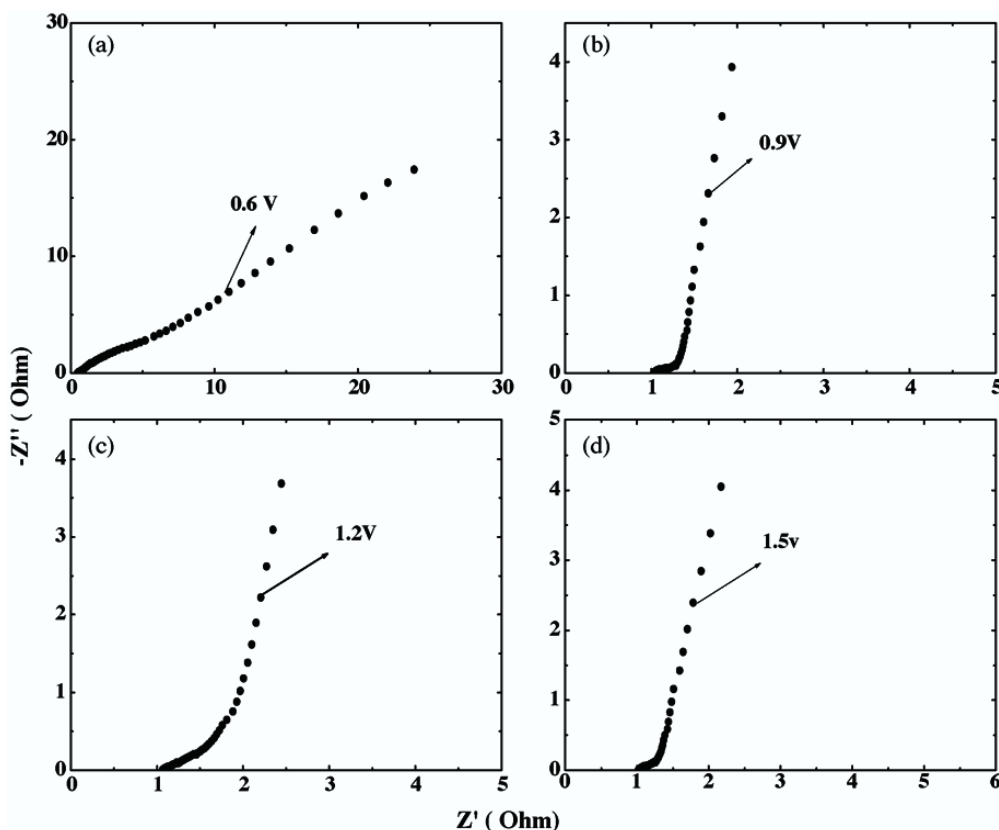


Figure 4. Typical electrochemical impedance spectroscopy of the hybrid supercapacitor at different applied potentials (Reproduced with permission from ref. [35]).

The Nyquist plots were plotted as Z_{im} versus Z_{re} in acid/alkaline medium using the frequency range from higher to lower [35]. A well defined semi-circle region at the high frequency range and a straight line appears at a low frequency range measured for both modified and unmodified electrode. The diameter of the semi-circle represents the interfacial charge transfer of faradaic resistance (R_{ct}). A decrease in faradaic resistance renders the value of power density increases [36]. The electrochemical impedance spectroscopy can be used to measure the specific capacitance values from the semi-circle region. The plot through 45° phase angle corresponds to the Warburg impedance and it indicates a high ion diffusion resistance.

The specific capacitance value has been evaluated from the following impedance spectroscopy equation (3) [37, 38]. When high frequency resistance was applied, which corresponds to the effective series resistance (ESR) of the supercapacitor, it showed highest ESR and electrode materials resistance and got highest specific capacitance value.

$$C_m = \frac{1}{m \times j \times 2\pi f \times Z''} \text{ F g}^{-1} \quad (3)$$

Where C_m denotes the specific capacitance from impedance spectra and Z'' imaginary part and f is the frequency; m is the mass of the active electrode materials. Wang *et al* [35] used the electrochemical impedance technique within the cyclic voltammetry potential window (0.6, 0.9, 1.0 and 1.2 V) in the applied frequency range 10^5 to 10^{-2} Hz, as shown in fig. 4.

4. PARAMETERS IN SUPERCAPACITORS

4.1 Columbic efficiency (η)

It is defined as the ratio of discharging time and charging time and it can be calculated by the following equation (4) [39-43].

$$\eta = \frac{t_D}{t_C} \times 100\% \quad (4)$$

Where η is columbic efficiency, t_D is discharging time (s), t_C is charging time (s). The columbic efficiency is calculated by cyclic stability method, by comparing the first and the end cycle. Khomenko *et al* [44] have discussed about the specific capacitance and its columbic efficiency. Here, as the specific capacitance value increases, the columbic efficiency decreases up to applied higher voltage (2V).

4.2. Power density (P) and Energy density (E)

Charge-discharge method is one of the well known methods to analyze the power density and energy density values of the supercapacitors. Notably, the energy density of supercapacitor decreases with increase in power density and therefore both of them have inverse relationship with each others. The energy density and power densities two parameters are very important tools for the investigation of electrochemical performance and its electrochemical cells. These kinds of parameters have been used to estimate the performance of working electrode materials. Energy density and power density were calculated from the following equations (5) and (6) [35, 36].

$$E = \frac{1}{2} C(\Delta V)^2 \quad (5)$$

$$P = \frac{E}{t} \quad (6)$$

Where C is specific capacitance ($F g^{-1}$), ΔV is potential window (V), t is discharge time (s), E is energy density ($Wh kg^{-1}$) and P is power density ($KW kg^{-1}$).

5. TYPES OF ELECTRODE MATERIALS FOR SUPERCAPACITORS

Different kind of electrode materials were prepared by different methods, especially nanostructured carbon based materials, transition metal oxides and conducting polymers. In the literature numerous efforts were made to develop these kinds of functional materials to get maximum power density supercapacitors.

5.1 Carbon based supercapacitors

Carbon materials have high surface area and can be used as electrical double layer capacitors. Different kinds of carbon materials are commercially available, such as powders, fibres, felts, monoliths and foils. The physical and chemical properties of carbon based materials such as single walled carbon nanotubes (SWCNT), multiwalled carbon nanotubes (MWCNT), fullerene and graphene are usually based on the carbon pore size which is about less than 1 nm. Only a few reviews in the literature have reported on the application of carbon based electrode materials in supercapacitor [45-49]. The activated nanoporous carbon has been used in supercapacitors applications with reported specific capacitance value of 240 F g^{-1} [50]. Merino *et al* [51] used activated carbon nanofibres as electrode material, which exhibited specific capacitance of about 60 F g^{-1} . Portet *et al* [52] evaluated activated carbon and carbon nanotube mixture in an organic electrolyte, which achieved the specific capacitance value of 90 F g^{-1} . Hwang *et al* [7] reported a specific capacitance value of about 220 F g^{-1} . Recently graphene based nanocomposite find widespread applications in diverse fields of research owing to their outstanding electronic properties. Recently, our research group reported various graphene based nanocomposite materials for the applications in sensors, biosensors, solar cells and biofuel cells [53-57]. In this way, number of graphene based composite materials were developed for the supercapacitors applications and they have shown significantly increased specific capacitances. Functionalized graphene sheets were synthesized by thermal exfoliation method and achieved the specific capacitance value of 230 F g^{-1} [58].

5.2. Metal oxides based supercapacitor

Generally metal oxides have been the mostly employed active electrode materials for the supercapacitors applications attributed to their exceptional physic-chemical properties. Various metal oxides, such as RuO_2 , MnO_2 , V_2O_5 , Fe_3O_4 and $\alpha\text{-Co(OH)}_2$ were aided in supercapacitors applications. Among these, amorphous RuO_2 is a promising electrode material with excellent electrochemical capacitance behavior. Ruthenium oxide has various forms like nanoneedles [59], nano-porous film [60] and nanoparticles [61]. Hu *et al* [62] have synthesized nanotubular array of $\text{RuO}_2 \cdot x\text{H}_2\text{O}$ by template method which exhibited a very high capacitance value of about 1300 F g^{-1} . Remarkably, Hydrous RuO_2 prepared by sol-gel method, showed a specific capacitance value of 390 F g^{-1} [63]. Similarly, chemically prepared RuO_2 exhibits a lowest capacitance value of 50 F g^{-1} [60]. Manganese oxide (MnO_2) has also been used as an electrode materials for supercapacitor applications. Wang *et al* [64] have prepared $\alpha\text{-MnO}_2$ electrode and the electrode surface area of $284 \text{ m}^2 \text{ g}^{-1}$ was obtained. The three-dimensional MnO_2 electrode material showed a specific capacitance of 200 F g^{-1} . On the other hand, amorphous nanostructured MnO_2 electrode has been synthesized by the mixing of KMnO_4 with ethylene glycol under ambient conditions and it shown much stability up to 1200 cycles 250 F g^{-1} of capacitance [65]. 2D nanosheets of MnO_2 have been prepared by exfoliation-reassembling method [66] which achieved the specific capacitance value of about $140\text{-}160 \text{ F g}^{-1}$ and the cyclic stability of $\sim 93\text{-}99\%$ up to 1000 cycles.

5.3. Conducting polymer based supercapacitor

Conducting polymers are interesting electrode materials for the supercapacitors applications. Conducting polymers can make stable double-layer capacitors due to change in their physical structure caused by doping/de-doping of ions [67]. Ghennatian *et al* [68] have prepared self-doped Polyaniline nanofibres by reverse pulse voltammetry method and observed the specific capacitance value of about 480 F g^{-1} . Sharma *et al* [69] reported the synthesis of polypyrrole film with specific capacitance value of 400 F g^{-1} . Poly(3,4-ethylenedioxythiophene) (PEDOT) has been synthesized by electrochemical method and achieved the specific capacitance of 130 F g^{-1} [70]. Polyaniline has been doped with para-toluene sulfonic acid by using potentiodynamic method [71]. The specific capacitance value of 405 F g^{-1} has been found by both cyclic voltammetry and electrochemical impedance spectroscopy methods.

5.4. Nanocomposites based electrode materials for supercapacitor

In general, the composite materials consist of the combination of two or more in which each individual component exhibit its unique chemical, mechanical and physical properties. Some literature have reported the modified electrode (composites) of carbon based material with conducting polymers [72] and metal oxides [16] etc. Yan *et al* [73] have prepared $\text{RuO}_2/\text{MWCNT}$ composite that exhibited specific capacitance value of 494 F g^{-1} from cyclic voltammetric method at lowest scan rate of 50 mV s^{-1} . The same kind of $\text{RuO}_2/\text{Multi-wall carbon nanotube (MWCNT)}$ has been synthesized by Liu and co-workers [74] and has maximum specific capacitance value of about $803 \pm 72 \text{ F g}^{-1}$. Coconut-shell carbon/ $\text{RuO}_x(\text{OH})_y$ composite with a specific capacitance value of 250 F g^{-1} has been prepared by simple sonication method [75]. Polyaniline/nafion/hydrous RuO_2 composite has been prepared by chemical method and obtained the reported specific capacitance value of 475 F g^{-1} [76]. A ternary composite of $\text{CNT/polypyrrole/MnO}_2$ has been prepared by Sivakkumar and co-workers [77] using *in situ* chemical method. The specific capacitance value of 281 F g^{-1} was obtained and it has excellent cyclic stability up to 10,000 cycles with only 12 % drop from the initial capacitance value. Graphene- MnO_2 nanocomposite electrode materials have recently attracted the self-limiting deposition of nano MnO_2 on the surface of graphene under microwave conditions [78] and reported specific capacitance value of 310 F g^{-1} at 2 mV s^{-1} .

5.5. Carbon-polymer based composites

Generally, carbon nanomaterials are used as an electrical double layer capacitor (EDLC). Instead, conducting polymers and metal oxides have been used to test pseudo-capacitance behavior. The composites with pseudo-capacitance properties of conducting polymers (polyaniline, polythiophen and polypyrrole) were embedded with electrical double layer capacitance properties of carbon nanomaterials (carbon fibre, MWCNT, fullerene and graphene). Mesoporous carbon/poly pyrrole composite has exhibited specific capacitance value of 487 F g^{-1} [79]. Yang *et al* [80] demonstrated a novel kind of PANI-CNTs composite, which exhibited a specific capacitance value of 163 F g^{-1} at a current density of 1 A g^{-1} . The other type of *in situ* polymerization composite of polyaniline/multi-

walled carbon nanotube showed the highest specific capacitance value of about 560 F g^{-1} [81]. Other authors [82] have reported the specific capacitance value of 180 F g^{-1} for polyaniline/porous carbon composite electrode materials. Recently, graphene oxide/PANI composite has been evaluated by Wang and co-workers [83], the reported specific capacitance value being about 531 F g^{-1} . From the above polymer composites, only polyaniline/multi-walled carbon nanotube electrode got highest specific capacitance value.

5.6. Carbon-metal oxide based composites

Carbon material has high surface area and regular pore structures, because of which it makes a composite material with metal oxides (like RuO_2 , MnO_2 and Fe_2O_3) very easily, and also it has both ionic and electronic conductivity of the electrode surface. The composite electrode materials exhibit high energy density and stable power densities. Mitra *et al* [17] have evaluated the exfoliated graphite-ruthenium oxide composite by sol-gel method and reported the specific capacitance value of about 176 F g^{-1} . Many authors have prepared carbon based manganese oxide composites like ZnO /carbon aerogel [84], MnO_2 /carbon [85], asymmetric carbon/ α - MnO_2 [86] and MnO_2 /CNTs embedded carbon nanofiber [87]. The above metal oxide composites have been reported for different specific capacitance values, such as 500, 458, 235 and 374 F g^{-1} respectively. Especially, manganese nano flower/carbon nanotube array have been synthesized by electrodeposition method and it exhibited specific capacitance value of 305 F cm^{-3} [88]. Zinc oxide/reduced graphene oxide composite is one of the novel electrode materials for very good capacitive behavior and it is found to have the specific capacitance value of 135 F g^{-1} [89].

5.7. Metal oxide-polymer based composites

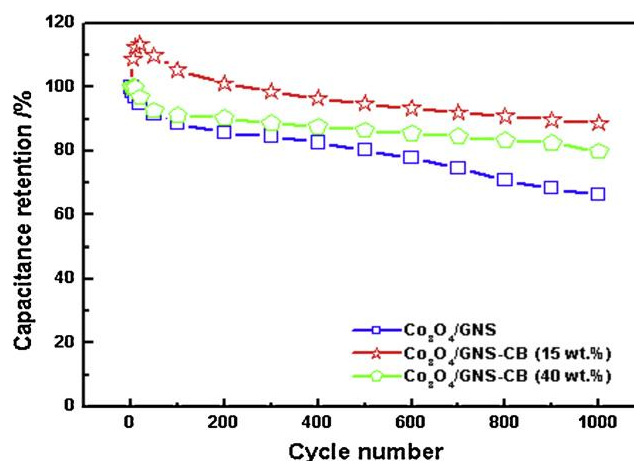


Figure 5. Cycle life of $\text{Co}_3\text{O}_4/\text{GNS}$, $\text{Co}_3\text{O}_4/\text{GNS-CB}$ (15 wt %) and $\text{Co}_3\text{O}_4/\text{GNS-CB}$ (40 wt %) (Reproduced with permission from ref. [85]).

Incorporation of metal oxides with conducting polymers are called composites. This is to improve their electrochemical properties. Among these transition metal oxides, hydrous ruthenium

oxide has best electrochemical capacitor properties than others. The electropolymerization of polyaniline/titanium oxide nano composite has been conducted by Mujawar and co-workers [90] with a specific capacitance value of about 740 F g^{-1} . Song *et al* [76] used the polyaniline/nafion/hydrous RuO_2 composite electrode to evaluate its specific capacitance behavior and reported maximum specific capacitance value of 475 F g^{-1} . Sharma and co-workers [14] found that electrochemically synthesized MnO_2/Ppy composite electrode exhibited a large specific capacitance value of 620 F g^{-1} . PANI/ MnO_2 composite has been evaluated by Chen and co-workers [12] who reported the specific capacitance value of 80 F g^{-1} and its stable columbic efficiency of about 98 % up to 1000 cycles.

6. STABILITY OF THE ELECTRODE

The cyclic stability of the electrode materials is a crucial and important parameter to rank the performances of the energy storage applications. Some of the reported literatures [35, 38] are discussed about the cyclic stability of electrodes and the loss of capacitance value after prolonged cycles. In fig. 5, the multiple cycle stability of cobalt/graphene nanosheet [91] was evaluated by cyclic voltammetry up to 1000 cycles, where the applied potential range is from -0.1 V to 0.35 V. At the end of 1000 cycles, $\text{Co}_3\text{O}_4/\text{GNS-CB}$ (15 wt %) composite electrode retained 89% of its specific capacitance validated the excellent stability of the composite film.

7. CONCLUSIONS

On the whole, supercapacitors have emerged as an important alternative energy technology with superior electrochemical properties, high energy density and good cyclic stability. Due to the high surface area, low porosity, high thermal and electrochemical conductivity, carbon materials (CNT, MWCNT, carbon nanofibres and activated carbon) have shown greatly improved supercapacitance performances. The highest specific capacitance value of activated nanoporous carbon is about 240 F g^{-1} . Though some of the carbon materials exhibited low specific capacitance and high energy density, their specific capacitance can be enhanced by the incorporation of metal oxides or conducting polymers in the activated carbon electrode materials. Polyaniline/multi-walled carbon nanotubes exhibited the highest specific capacitance value of 560 F g^{-1} among all the polymers based supercapacitors. ZnO/carbon aerogel achieved the highest specific capacitance value of about 500 F g^{-1} among all the metal oxides related composites. In conclusion, future efforts should focus on cheap electrode materials obtained using simple fabrication processes.

ACKNOWLEDGEMENT

This work was financial supported by the Council for Scientific and Industrial Research, New Delhi, India is gratefully acknowledged. This research work was supported by National Science Council, Taiwan and India-Taiwan Science and Technology Cooperation program, DST, India.

References

1. B.E. Conway, (1999) *Electrochemical supercapacitors, scientific fundamentals and technological applications*, Plenum, New York.
2. A. Burke, *J. Power Sources*, 91 (2000) 37.
3. L.L. Zhang, X.S. Zhao, *Chem. Soc. Rev.*, 38 (2009) 2520.
4. M. Yu, Y.M. Volfkovich, T.M. Serdyuk, *Russ. J. Electrochem.*, 38 (2002) 935.
5. R. Kotz, M. Carlen, *Electrochim. Acta*, 45 (2000) 2483.
6. A. Janes, H. Kurig, E. Lust, *Carbon*, 45 (2007) 1226.
7. S.W. Hwang, S.H. Hyun, *J. Nano-crystalline Solids*, 347 (2004) 238.
8. X. Zhao, H. Tian, M. Zhu, K. Tian, J.J. Wang, F. Kang, R.A. Outlaw, *J. Power Sources*, 194 (2009) 1208.
9. E. Frackowiak, K. Jurewicz, K. Szostak, S. Delpeux, F. Beguin, *Fuel Process. Technol.*, 77 (2002) 213.
10. J. Yan, T. Wei, W. Qiao, Z. Fan, L. Zhang, T. Li, Q. Zhao, *Electrochem. Commun.*, 12 (2010) 1279.
11. T. Liu, W.G. Pell, B.E. Conway, *Electrochim. Acta*, 42 (1997) 3541.
12. L. Chen, L.J. Sun, F. Luan, Y. Liang, Y. Li, X.X. Liu, *J. Power Sources*, 195 (2010) 3742.
13. L.J. Bian, J.H. Zhang, J. Qi, X.X. Liu, D. Dermot, K.T. Lau, *Sens. Actuators, B*, 147 (2010) 73.
14. R.K. Sharma, A.C. Rastogi, S.B. Desu, *Electrochim. Acta*, 53 (2008) 7690.
15. J. Yan, Z. Fan, T. Wei, W. Qian, M. Zhang, F. Wei, *Carbon*, 48 (2010) 3825.
16. Y. Zhang, H. Li, L. Pan, T. Lu, Z. Sun, *J. Electroanal. Chem.*, 634 (2009) 68.
17. S. Mitra, K.S. Lokesh, S. Sampath, *J. Power Sources*, 185 (2008) 1544.
18. L. Peng, Y. Feng, P. Lv, D. Lei, Y. Shen, Y. Li, W. Feng, *J. Phys. Chem., C* 116 (2012) 4970.
19. Y. Lin, N. Zhao, W. Nie, X. Ji, *J. Phys. Chem. C*, 112 (2008) 16219.
20. M. Wu, J. Gao, S. Zhang, A. Chen, *J. Power Sources*, 159 (2006) 365.
21. K.S. Ryu, M.K. Kim, N.G. Park, J.Y. Park, S.H. Chang, *J. Power Sources*, 103 (2002) 305.
22. W. Sun, X. Chen, *J. Power Sources*, 193 (2009) 924.
23. H. Li, R. Wang, R. Cao, *Microporous Mesoporous Mater.*, 111 (2008) 32.
24. J.H. Jang, A. Kato, K. Machida, K. Naoi, *J. Electrochem. Soc.* 153 (2006) A321.
25. X. Zhao, C. Johnston, P.S. Grant, *J. Mater. Chem.*, 19 (2009) 8755.
26. J. Liu, J. Essner, J. Li, *Chem. Mater.*, 22 (2010) 5022.
27. Z. Li, J. Wang, S. Liu, X. Liu, S. Yang, *J. Power sources*, 196 (2011) 8160.
28. Z. Yang, C.Y. Chen, H.T. Chang, *J. Power Sources*, 196 (2011) 7874.
29. M. Xu, L. Kong, W. Zhou, H. Li, *J. Phys. Chem. C*, 111 (2007) 19141-19147.
30. C.C. Wang, C.C. Hu, *Carbon*, 43 (2005) 1926.
31. J.W. Choi, J. McDonough, S. Jeong, J.S. Yoo, C.K. Chan, Y. Cui, *Nano Lett.*, 10 (2010) 1409.
32. H. Wang, Y. Liang, T. Mirfakhrai, Z. Chen, H.S. Casalongue, H. Dai, *Nano Res.* 4 (2011) 729.
33. A.M. Polaczyk, C.V. Guterl, E. Frackowiak, *Energy Fuels*, 24 (2010) 3346.
34. N. Tang, X. Tian, C. Yang, Z. Pi, *Mater. Res. Bull.*, 44 (2009) 2062.
35. Y.G. Wang, L. Cheng, Y.Y. Xia, *J. Power Sources*, 153 (2006) 191.
36. Y.G. Wang, Z.D. Wang, Y.Y. Xia, *Electrochim. Acta*, 50 (2005) 5641.
37. J. Zang, S.J. Bao, C.M. Li, H. Bian, X. Cui, Q. Bao, C.Q. Sun, J. Guo, K. Lian, *J. Phys. Chem. C*, 112 (2008) 14843.
38. Y.Y. Liang, H.L. Li, X.G. Zhang, *J. Power Sources*, 173 (2007) 599.
39. J.H. Parka, J.M. Kob, O.O. Parka, D.W. Kimb, *J. Power Sources*, 105 (2002) 20.
40. V. Ganesh, S. Pitchumani, V. Lakshminarayanan., *J. Power Sources*, 158 (2006) 1523.
41. G. Wang, M. Qua, Z. Yu, R. Yuan, *Mater. Chem. and Phys.*, 105 (2007) 169.
42. M.D. Stoller, R.S. Ruoff, *Energy Environ. Sci.*, 3 (2010) 1294.
43. S. Mallika, R. Saravana Kumar, *Int. J. Eng. Sci. Tech.*, 3 (2011) 37.

44. V. Khomenko, E.R. Pi, F. Beguin, *J. Power Sources*, 153 (2006) 183.
45. E. Frackowiak, F. Beguin, *Carbon*, 39 (2001) 937.
46. E. Frackowiak, *Phys. Chem. Chem. Phys.*, 9 (2009) 1774.
47. V.V.N. Obreja, *Physica E*, 40 (2008) 2596.
48. M. Pumera, *Energy Environ. Sci.*, 4 (2011) 668.
49. R. Ramachandran, V. Mani, S.-M. Chen, R. Saraswathi, B.-S. Lou, *Int. J. Electrochem. Sci.*, 8 (2013) 11680.
50. A. Janes, H. Kurig, E. Lust., *Carbon*, 45 (2007) 1226.
51. C. Merino, P. Soto, E.V. Ortego, J.M.G. Salazar, F. Pico, J.M. Rojo, *Carbon*, 43 (2005) 551.
52. C. Portet, P.L. Taberna, P. Simon, E. Flahaut, *J. Power Sources*, 139 (2005) 371.
53. V. Mani, A.P. Periasamy, S.-M. Chen, *Electrochem. Commun.*, 17 (2012) 75.
54. B. Unnikrishnan, S. Palanisamy, S.-M. Chen, *Biosens. Bioelectron.*, 39 (2013) 70.
55. Y. Umasankar, B. Unnikrishnan, S.-M. Chen, T.-W. Ting, *Anal. Methods*, 4 (2012) 3653.
56. B. Devadas, V. Mani, S.-M. Chen, *Int. J. Electrochem. Sci.*, 7 (2012) 8064.
57. T.-H. Tsai, S.-C. Chiou, S.-M. Chen, *Int. J. Electrochem. Sci.*, 6 (2011) 3333.
58. Q. Du, M. Zheng, L. Zhang, Y. Wang, J. Chen, L. Xue, W. Dai, G. Ji, J. Cao, *Electrochim. Acta*, 55 (2010) 3897.
59. M. Subhramannia, B.K. Balan, B.R. Sathe, I.S. Mulla, V.K. Pillai, *J. Phys. Chem. C*, 111 (2007) 16593.
60. V.D. Patake, C.D. Lokhande, *App. Surf. Sci.*, 254 (2008) 2820.
61. A. Devadas, S. Baranton, T.W. Napporn, C. Coutanceau, *J. Power Sources*, 196 (2011) 4044.
62. C.C. Hu, K.S. Chang, M.C. Lin, Y.T. Wu, *Nano. Lett.* 6 (2006) 2690.
63. K.H. Chang, C.C. Hu, C.Y. Chou, *Electrochim. Acta* 54 (2009) 978.
64. Y.T. Wang, A.H. Lu, H.L. Zhang, W.C. Li, *J. Phys. Chem. C*, 115 (2011) 5413.
65. P. Regupathy, D.H. Park, G. Campet, H.N. Vasan, S.J. Hwang, J.H. Choy, N. Munichandraiah, *J. Phys. Chem. C*, 113 (2009) 6303.
66. M.S. Song, K.M. Lee, Y.R. Lee, I.Y. Kim, T.W. Kim, J.L. Gunjekar, S.J. Hwang, *J. Phys. Chem. C*, 114 (2010) 22134.
67. G.A. Snook, P. Kao, A.S. Best, *J. Power Sources*, 196 (2011) 1.
68. H.R. Ghennatian, M.F. Mousavi, S.H. Kazemi, M. Shamsipur, *Syn. Metals*, 159 (2009) 1717.
69. R.K. Sharma, A.C. Rastogi, S.B. Desu, *Electrochem. Commun.*, 10 (2008) 268.
70. K. Liu, Z. Hu, R. Xue, J. Zhang, J. Zhu., *J. Power Sources*, 179 (2008) 858.
71. T.C. Girija, M.V. Sangaranarayanan, *J. Power Sources*, 156 (2006) 705.
72. C. Peng, S. Zhang, D. Jewell, C.Z. Chen, *Prog Nat. Sci.*, 18 (2008) 777.
73. S. Yan, H. Wang, P. Qu, Y. Zhang, Z. Xiao, *Syn. Metal.*, 159 (2009) 158.
74. X. Liu, T.A. Huber, M.C. Kopac, P.G. Pickup, *Electrochim. Acta*, 54 (2009) 7141.
75. M.S. Dandekar, G. Arabale, K. Vijayamohanan, *J. Power Sources*, 141 (2005) 198.
76. R.Y. Song, J.H. Park, S.R. Sivakkumar, S.H. Kim, J.M. Ko, D.Y. Park, S.M. Jo, D.Y. Kim, *J. Power Sources*, 166 (2007) 297.
77. S.R. Sivakkumar, J.M. Ko, D.Y. Kim, B.C. Kim, G.G. Wallace, *Electrochim. Acta*, 52 (2007) 7377.
78. J. Yan, Z. Fan, T. Wei, W. Qian, M. Zhang, F. Wei, *Carbon*, 48 (2010) 3825.
79. J. Zhang, L.B. Kong, J.J. Cai, Y.C. Luo, L.L. Kang, *Electrochim. Acta*, 55 (2010) 8067.
80. M. Yang, B. Cheng, H. Song, X. Chen, *Electrochim. Acta*, 55 (2010) 7021.
81. Y. Zhou, Z.Y. Qin, L. Li, Y. Zhang, Y.L. Wei, L.F. Wang, M.F. Zhu, *Electrochim. Acta*, 55 (2010) 3904.
82. W.C. Chen, T.C. Wen, H. Teng, *Electrochim. Acta*, 48 (2003) 641.
83. H. Wang, Q. Hao, X. Yang, L. Lu, X. Wang, *Electrochem. Commun.*, 11 (2009) 1158.
84. D. Kalpana, K.S. Omkumar, S. Suresh Kumar, N.G. Renganathan, *Electrochim. Acta*, 52 (2006) 1309.

85. R.K. Sharma, H.S. Oh, Y.G. Shul, H. Kim, *J. Power Sources*, 173 (2007) 1024.
86. A.J. Roberts, R.C.T. Slade, *Electrochim. Acta*, 55 (2010) 7460.
87. J.G. Wang, Y. Yang, Z.H. Huang, F. Kang, *Electrochim. Acta*, 75 (2012) 213.
88. H. Zhang, G. Cao, Z. Wang, Y. Yang, Z. Shi, Z. Gu, *Nano Lett.*, 8 (2008) 2664.
89. Y.L. Chen, Z.A. Hu, Y.Q. Chang, H.W. Wang, Z.Y. Zhang, Y.Y. Yang, H.Y. Wu, *J. Phys. Chem. C*, 115 (2011) 2563.
90. H.S. Mujawar, S.B. Ambade, T. Battumur, R.B. Ambade, S.H. Lee, *Electrochim. Acta*, 56 (2011) 4462.
91. S. Park, S. Kim, *Electrochim. Acta*, 89 (2013) 516.

© 2014 The Authors. Published by ESG (www.electrochemsci.org). This article is an open access article distributed under the terms and conditions of the Creative Commons Attribution license (<http://creativecommons.org/licenses/by/4.0/>).